Available online at www.sciencedirect.com
ScienceDirect
International Journal of Mass Spectrometry 267 (2007) 220–232
International Journal of Mass Spectrometry
www.elsevier.com/locate/ijms

Experimental and theoretical proton affinities of methionine, methionine sulfoxide and their N- and C-terminal derivatives☆

Hadi Lioe[a,b], Richard A.J. O'Hair[a,b,*], Scott Gronert[c,**], Allen Austin[c], Gavin E. Reid[d,e,***]

[a] *School of Chemistry, University of Melbourne, Victoria 3010, Australia*
[b] *Bio21 Institute of Molecular Science and Biotechnology, University of Melbourne, Victoria 3010, Australia*
[c] *Department of Chemistry and Biochemistry, San Francisco State University, San Francisco, CA 94132, United States*
[d] *Department of Chemistry, Michigan State University, East Lansing, MI 48824, United States*
[e] *Department of Biochemistry and Molecular Biology, Michigan State University, East Lansing, MI 48824, United States*

Received 2 October 2006; received in revised form 16 February 2007; accepted 21 February 2007
Available online 25 February 2007

Dedicated to the memory of Sharon G. Lias.

Abstract

The proton affinities of methionine, methionine sulfoxide and their derivatives (methionine methyl ester, methionine sulfoxide methyl ester, methionine methyl amide, methionine sulfoxide methyl amide, *N*-acetyl methionine, *N*-acetyl methionine sulfoxide, *N*-acetyl methionine methyl ester, *N*-acetyl methionine sulfoxide methyl ester, *N*-acetyl methionine methyl amide and *N*-acetyl methionine sulfoxide methyl amide) were experimentally determined using the kinetic method, in which proton bound dimers formed via electrospray ionization (ESI) were subjected to collision induced dissociation (CID) in a triple quadrupole mass spectrometer. In addition, theoretical calculations carried out at the MP2/6-311 + G(2d,p)//B3LYP/6-31 + G(d,p) level of theory to determine the global minima of the neutral and protonated species of all derivatives studied, were used to predict theoretical proton affinities. The density function theory calculations not only support the experimental proton affinities, but also provide structural insights into the types of hydrogen bonding that stabilize the neutral and protonated methionine or methionine sulfoxide derivatives. Comparison of the proton affinities of the various methionine and methionine sulfoxide derivatives reveals that: (i) oxidation of methionine derivatives to methionine sulfoxide derivatives results in an increase in proton affinity due to higher intrinsic proton affinity and an increase in the ring size formed through charge complexation of the sulfoxide group, which allows more efficient hydrogen bonding compared to the sulfide group; (ii) C-terminal modification by methyl esterification or methyl amidation increases the proton affinity in the order of methyl amide > methyl ester > carboxylic acid due to improved charge stabilization; (iii) N-terminal modification by *N*-acetylation decreases proton affinity of the derivatives due to lower intrinsic proton affinity of the *N*-acetyl group as well as due to stabilization of the attached proton by only one functional group (instead of two functional groups in derivatives containing a free amino group); and (iv) a combination of the above methionine modifications is observed to affect the proton affinity in an additive way. While a number of factors might contribute to discrepancies between the theoretical and experimental proton affinities, a key factor may be that the global minimum of the neutral species is further stabilized by strong intramolecular hydrogen bonding, and this particular conformer may not be sampled during dissociation of the proton bound dimer.

Keywords: Proton affinity; Amino acid; Methionine sulfoxide; Kinetic method; DFT calculations

1. Introduction

Thermochemical properties such as proton affinities and metal ion affinities are important fundamental properties [1] associated with the gas phase chemistry of bio-ions and can be used to evaluate ionization mechanisms (e.g., in matrix-assisted laser desorption ionization [2]). In peptide sequencing via tandem mass spectrometry, the relative proton affinities of amino

☆ This paper is Part 53 of the series "Gas Phase Ion Chemistry of Biomolecules".

* Corresponding author. Tel.: +61 3 8344 6490; fax: +61 3 9347 5180.
** Corresponding author. Tel.: +1 415 338 7709; fax: +1 415 338 2384.
*** Corresponding author. Tel.: +1 517 355 9715; fax: +1 517 353 1793.
E-mail addresses: rohair@unimelb.edu.au (R.A.J. O'Hair), sgronert@sfsu.edu (S. Gronert), reid@chemistry.msu.edu (G.E. Reid).

1387-3806/$ – see front matter.
doi:10.1016/j.ijms.2007.02.038

acids have been used as a basis for the "mobile proton" model of peptide ion fragmentation [3,4]. Since arginine has the highest proton affinity of any amino acid, a simple comparison of the number of arginine residues (x) within a peptide to the number of ionizing protons (n) in the $[M+nH]^{n+}$ precursor ion dictates whether the peptide ion will fragment under mobile proton conditions. If $x<n$, then the proton(s) is mobile and the peptide ion will fragment via charge directed processes, which often involve neighbouring group reactions [5]. In contrast, if $x \geq n$, then the ionizing protons are sequestered by the arginine side chain(s) yielding a non-mobile proton condition in which the peptide ion is more likely to fragment via charge remote processes (such as aspartic acid cleavages [6]). Furthermore, the relative proton affinities of the products formed by MS/MS determines which peptide fragment ion (N- or C-terminal) is observed after bond cleavage of the $[M+H]^+$, as demonstrated by Morgan and Bursey [7,8].

As models for predicting peptide fragmentation become more sophisticated, they will require new thermochemical data. For example, post-translational modification of an amino acid residue will clearly change its proton affinity and may lead to a change in fragmentation chemistry. A clear manifestation of the effects of post-translational modification is observed in the fragmentation behavior of protonated peptide ions containing methionine sulfoxide [9,10]. In the case of charge-directed fragmentation, peptide ions containing methionine sulfoxide residues fragment at higher energy than their non-oxidized methionine-containing peptide ion counterparts. This observation may be explained if the intrinsic proton affinity of the methionine sulfoxide residue is higher than that of methionine, hence causing ionizing protons to be "less-mobile" [10].

A key question that has largely been neglected is "do the relative proton affinities of amino acids reflect the relative "local" proton affinities of amino acid residues within peptides, or should better model systems be sought?" Siu and co-workers studied a number of *N*-acetyl amino acid methyl esters and found that the proton affinity of this simple peptide model is consistently higher than that of the amino acid [11]. It was suggested that this is due to greater stabilization of the protonated *N*-acetyl amino acid methyl esters system by intramolecular ionic hydrogen bonding between the N- and C-termini of the molecule. On the other hand, equilibrium measurements by Kinser et al. [12] found that lysine amide has a similar proton affinity to that of lysine [13]. These studies suggest that the site of proton attachment and the degree of charge stabilization/delocalization are important factors which determine the "local" proton affinity of an amino acid residue.

The focus of this work is to determine proton affinity values for methionine (Met), methionine sulfoxide (Met(O)), and to see how these properties change as simple modifications are made at the N- and/or C-terminus. We use the simple kinetic method using amino acids as reference bases (see Section 2 for more details), as well as theoretical calculations (density functional theory (DFT) and ab initio) to gain structural insights into how intramolecular hydrogen bonding influences the proton affinity.

2. Experimental

2.1. Materials

Amino acids were purchased from Sigma Co. (St. Louis, USA). Methionine *O*-methyl ester, *N*-acetyl methionine and *N*-acetyl methionine *O*-methyl ester, were obtained from BACHEM (Bubendorf, Switzerland). Methanol (ChromAR grade) was purchased from Mallinkrodt (Melbourne, Australia). Acetic acid was obtained from Merck (Darmstadt, Germany). Hydrogen peroxide (30% aqueous solution) was purchased from Merck. Methyl amine (30% aqueous solution) was purchased from Ajax Chemicals Pvt. Ltd. (NSW, Australia). All reagents were used without further purification.

2.2. Oxidation of methionine derivatives

Lyophilized Met derivatives (1 mg) were dissolved in 50 μL of 50% CH_3OH/50% H_2O containing 0.1 M acetic acid. Then, 50 μL of 30% aqueous hydrogen peroxide was added and the reaction was allowed to proceed at room temperature for 15 min. The mixture was dried by lyophilization, and used without further purification. Based on the ESI/MS precursor ion abundances of the Met(O) derivatives, the reaction had proceeded to near completion (>98%).

2.3. Methyl amidation of methionine derivatives

We have used the method of Feenstra et al. [14] for methyl amidation of methionine derivatives. Briefly, the methyl ester of methionine derivatives (2 mg) were dissolved in 1 mL of 30% CH_3NH_2/H_2O and the reaction was allowed to proceed at room temperature for 30 min. The mixture was dried by lyophilization, dissolved in 50% CH_3OH/50% H_2O containing 0.1 M acetic acid, and then lyophilized again. The methyl amide was used without further purification.

2.4. Mass spectrometry

All experiments were carried out using electrospray ionization (ESI) on a triple quadrupole mass spectrometer (model TSQ, Finnigan, San Jose, CA, USA). To form proton bound dimers, each of the amino acid and model peptide derivatives (1 mM) in 50% CH_3OH/50% H_2O containing 0.1 M acetic acid were mixed with equimolar amounts of the reference base prior to introduction to the mass spectrometer at 5 μL min^{-1} via an external syringe pump. The spray voltage was set at 4.5 kV. Nitrogen sheath gas was supplied at 25 psi. The heated capillary temperature was 200 °C. For MS/MS experiments, each proton bound dimer was subjected to collision energies between 7 and 15 V (laboratory scale) at 1 V increments. For simple kinetic method analysis, proton affinity values are reported using collision energy of 10 V (laboratory scale). Thirty product ion scans were acquired at each collision energy. The collision pressure was maintained at 0.75 mTorr for all experiments. All experiments were performed three times for proper statistical analysis.

2.5. Overview of the kinetic method employed

The kinetic method initially developed by Cooks and co-workers, which is a form of a thermokinetic method to determine proton affinity was employed in the present work [15–18]. The kinetic method, works on the basis of competitive fragmentation of a proton bound dimer ([M-H-B]$^+$) to form the respective protonated monomers depending on their relative proton affinity (Eqs. (1) and (2)) [16,18].

$$[\text{M-H-B}]^+ \rightarrow [\text{MH}]^+ + \text{B} \quad (1)$$

$$[\text{M-H-B}]^+ \rightarrow [\text{BH}]^+ + \text{M} \quad (2)$$

The ratio of the rate constant for these two dissociation pathways can be expressed as:

$$\ln\frac{k_1(T)}{k_2(T)} = -\frac{\Delta_1 E_0^{\ddagger} - \Delta_2 E_0^{\ddagger}}{RT} + \ln\frac{Q_1^{\ddagger}(T)}{Q_2^{\ddagger}(T)} \quad (3)$$

where $\Delta_j E_0^{\ddagger}$ is the activation barrier and $Q_j^{\ddagger}(T)$ is the partition function for the transition state for dissociation of the proton bound dimer to path j ($j = 1$ or 2).

Common assumptions in the kinetic method are: (a) the ratio of product ion abundances are approximately equal to the ratio of the rate constants [$I_M/I_B \approx k_1(T)/k_2(T)$], (b) the absence of (or equal) reverse activation barriers for both pathways such that $\Delta_j E_0^{\ddagger} = \Delta_j E_0$ (or $\Delta\Delta E_0^{\ddagger} = \Delta\Delta E_0 = \Delta_1 E_0 = \Delta_2 E_0$), (c) the difference in protonation energy can be approximated by the difference in proton affinity [$-(\Delta_1 E_0 - \Delta_2 E_0) \approx \text{PA}_M - \text{PA}_B$], (d) the above Eq. (3) holds true even when the system is not under thermal equilibrium, (e) the absence of secondary fragmentation within the proton bound dimer or the protonated monomeric product ions, and (f) the protonation entropy difference in both pathways is zero [$\Delta(\Delta S^{\ddagger}(T)) = R\ln(Q_1^{\ddagger}/Q_2^{\ddagger}) \approx 0$]. When these assumptions apply, the above Eq. (3) may then be simplified to:

$$\ln\frac{I_M}{I_B} = \frac{\text{PA}_M - \text{PA}_B}{RT_{\text{eff}}} = \frac{\text{GB}_M - \text{GB}_B}{RT_{\text{eff}}} \quad (4)$$

To indicate that the system is not under thermal equilibrium, effective temperature, T_{eff} is used instead of equilibrium temperature, T. The meaning of T_{eff} has been discussed several times [19,20], and refers to "mean internal energy of ions that are dissociated during the time window of analysis" [19] and hence is directly proportional to the source temperature (for metastable ion mass spectrometry (MI)), or the collision energy (for collision induced dissociation (CID)). Proton affinity of the unknown can then be simply determined by dissociating proton bound dimer of the unknown (M) with a series of reference bases (B). The plot of $\ln(I_M/I_B)$ versus PA_B yields a straight line with a slope of $m_0 = -1/RT_{\text{eff}}$ and a y-intercept of $y_0 = \text{PA}_M/RT_{\text{eff}} = \text{GB}_M/RT_{\text{eff}}$ (PA_M can be evaluated from either the y-intercept, y_0, or directly from the x-intercept, x_0).

Wu and Fenselau [21,22] and Wesdemiotis and co-workers [23–25] modified the kinetic method such that both the enthalpy and the "apparent" entropy of protonation can be measured (known also as the extended kinetic method), provided that protonation entropy among the reference bases is a constant [$R\ln(Q_1^{\ddagger}/Q_2^{\ddagger}) = \Delta(\Delta S^{\ddagger}(T)) = \Delta(\Delta S(T)) = \text{constant}$] (similar structural features among the reference bases) (Eq. (5)).

$$\ln\frac{I_M}{I_B} = \frac{\text{PA}_M - \text{PA}_B}{RT_{\text{eff}}} + \frac{\Delta(\Delta S)}{R} \quad (5)$$

Armentrout further improved the extended kinetic method to statistically remove the covariance that exists between the slope and y-intercept during linear regression analysis of the first plot [26]. In this modification, Eq. (5) becomes Eq. (6).

$$\ln\frac{I_M}{I_B} = \frac{(\text{PA}_M - \text{PA}_{\text{avg}}) - (\text{PA}_B - \text{PA}_{\text{avg}})}{RT_{\text{eff}}} + \frac{\Delta(\Delta S)}{R} \quad (6)$$

In this version of the extended kinetic method (see Eq. (6)), dissociation of the proton bound dimer is conducted at different T_{eff} (either different source temperatures for MI or different collision energy for CID), and $\ln(I_M/I_B)$ is plotted against ($\text{PA}_B - \text{PA}_{\text{avg}}$) at various T_{eff}, where PA_{avg} is the average proton affinity of the reference bases used ($\Sigma\text{PA}_B/n$). The y-intercept ($y'_1 = (\text{PA}_M - \text{PA}_{\text{avg}})/RT_{\text{eff}} + \Delta(\Delta S)/R$) from the first plot is then plotted against the negative of the slope ($-m'_1 = 1/RT_{\text{eff}}$) (see Eq. (6)). From the second plot, PA_M and $\Delta(\Delta S)$ can be evaluated from the slope of the line ($m'_2 = (\text{PA}_M - \text{PA}_{\text{avg}})$) and the y-intercept ($y'_2 = \Delta(\Delta S)/R$), respectively. The second term ($\Delta(\Delta S)$), however, is not a true thermodynamic property [27].

2.6. Choice of proton affinity scale for reference bases

In this study, amino acids have been used as the reference bases for the kinetic method since attempts to use simple amine bases were unsuccessful due to an insufficient number of suitable reference bases at the high end of the gas phase basicity scale. Several scales of proton affinities of amino acids, determined by different methods such as the bracketing method by Gorman et al. [28], the equilibrium method by Meot-Ner et al. [29], the evaluated scale by Lias et al. [30], by Hunter and Lias [31], and by Harrison [32], the kinetic method by Bojesen and Breindahl [33], by Li and Harrison [34], and by Afonso et al. [35], the theoretical study by Maksic and Kovacevic [36] and very recently by Bleiholder et al. [37] have been described. The compilation by Hunter and Lias [31] is generally the most accepted. Since the publication of an evaluated proton affinity scale by Hunter and Lias, there have been numerous studies aimed at determining individual proton affinities of amino acids [38–45]. Several disagreements with absolute proton affinity values and the relative order of amino acid proton affinities from those reported in the Hunter and Lias list have been noted.

In the present investigation, we have employed the evaluated scale of amino acid proton affinities by Hunter and Lias [31] (this scale shall henceforth be referred to as the Hunter and Lias scale), the scale by Harrison [32] (henceforth be referred to as the Harrison scale), and the scale by Afonso et al. [35] (henceforth be referred to as the Tabet scale) to anchor our experimental results. The Hunter and Lias, Harrison and the Tabet scales of proton affinities were used when analysing Met and Met(O), while only the Tabet scale was used when analysing the other methionine and methionine sulfoxide derivatives. The decision

to use the Tabet scale for the derivatives was driven, in part, by a belief that it provides the most self-consistent set of apparent basicities for the amino acids. It is known that amino acids at the high end of the scale (e.g., Lys) form cyclic cations and therefore require significant corrections for their entropies of protonation. For some amino acids, these are not well established, so we have chosen to use the simple kinetic method analysis and report values from experiments at a constant collision energy (10 V lab frame). We will refer to the data as *apparent proton affinities* to highlight the fact that no entropy corrections were made and it is assumed that all the Met derivatives have similar entropies of protonation. However, it should be noted that we applied the extended kinetic method analysis to several of the Met derivatives whose basicity did not require using amino acid references with significant entropy of protonation corrections. The trends observed in these analyses parallel those observed in the simple kinetic method analyses (data not shown).

2.7. Error estimation for the kinetic method

There are two types of errors inherent in the present application of the kinetic method. First, there is uncertainty in the proton affinities of the reference bases, which includes at least a ± 1 kcal mol^{-1} contribution from the inherent uncertainty of the entire gas phase proton affinity scale as well as an estimated uncertainty of ± 2 kcal mol^{-1} for the lack of entropy corrections in the Tabet scale. This leads to expected, absolute uncertainties in the ± 3 kcal mol^{-1} range. In addition, uncertainties are generated in the plots used in the simple kinetic method. These are expected to be small and on the order of a few tenths of a kcal mol^{-1}. As always in proton affinity studies of this type, the uncertainties in relative values are expected to be much lower. Because similar structures are involved, the variations in entropies of protonation are expected to be small and favorable cancellation of other errors is likely. We anticipate uncertainties in the range of ± 1 kcal mol^{-1} in the relative values.

2.8. Computational methods

Initially, a Monte Carlo survey at the PM3 level was completed in Spartan02 to identify 100 likely candidates for the global minimum. Structures with an R- or S-configuration at the sulfoxide sulfur were considered. Each of the 100 structures was subjected to single-point calculations at the B3LYP level of theory with the standard 6-31 + G(d,p) basis set [46] using the GAUSSIAN 03 [47] molecular modeling package. The 10 best (lowest energy) conformations from these calculations then were optimized at the B3LYP/6-31 + G(d,p) level. Single point calculations were then performed at the MP2/6-311 + G(2d,p) level of theory to provide better relative energy calculations for compounds containing sulfur [48]. All optimized structures were subjected to vibrational frequency analysis (B3LYP/6-31 + G(d,p) level) and visualized using the computer package GaussView 3.0 [49] to determine the nature of the stationary points. The proton affinity of the methionine and methionine sulfoxide derivatives were calculated according to the negative of the enthalpy of the protonation reaction (7) via Eqs. (8)–(10),

$$\mathrm{M} + \mathrm{H}^+ \rightarrow \mathrm{MH}^+ \tag{7}$$

$$\mathrm{PA} = -\Delta_\mathrm{r} H^0_{298} \tag{8}$$

$$\Delta_\mathrm{r} H^0_{298} = \Delta_\mathrm{r} E + \Delta(\Delta E_{\mathrm{t},298}) + \Delta(\Delta E_{\mathrm{r},298}) + \Delta(\Delta E_{\mathrm{v},298}) + \Delta PV \tag{9}$$

where $\Delta_\mathrm{r} E = E_\mathrm{elec}(\mathrm{MH}^+) - E_\mathrm{elec}(\mathrm{M}) + \mathrm{ZPE}(\mathrm{MH}^+) - \mathrm{ZPE}(\mathrm{M})$. E_elec is the electronic energy of the species, ZPE the zero-point energy correction of the species, and $\Delta(\Delta E_{\mathrm{t},298})$, $\Delta(\Delta E_{\mathrm{r},298})$ and $\Delta(\Delta E_{\mathrm{v},298})$ are the difference in translational, rotational and vibrational energy correction (from 0 to 298 K) between the products and reactants, respectively. When $\Delta PV = -RT$ is assumed (ideal condition), $\Delta(\Delta E_{\mathrm{t},298}) = -3/2RT$ from the contribution of the proton and $\Delta(\Delta E_{\mathrm{r},298}) = 0$. $\Delta E_{\mathrm{v},298}(\mathrm{MH}^+)$, $\Delta E_{\mathrm{v},298}(\mathrm{M})$ and ZPE values are obtained from the output of structural optimization. Hence, Eq. (9) becomes:

$$\Delta_\mathrm{r} H^0_{298} = E_\mathrm{elec}(\mathrm{MH}^+) - E_\mathrm{elec}(\mathrm{M}) + \mathrm{ZPE}(\mathrm{MH}^+) - \mathrm{ZPE}(\mathrm{M}) + \Delta E_{\mathrm{v},298}(\mathrm{MH}^+) - \Delta E_{\mathrm{v},298}(\mathrm{M}) - \frac{5}{2}RT. \tag{10}$$

3. Results

3.1. Proton affinity of methionine and methionine sulfoxide determined using the Hunter and Lias scale, Harrison scale, and the Tabet scale of amino acid proton affinities

Table 1 lists the experimentally determined proton affinities of Met and Met(O) using both the simple and extended kinetic method relative to the Hunter and Lias, the Harrison and the Tabet scales. Using the simple kinetic method, the apparent proton affinity of Met was determined to be 221.5–221.6 kcal mol^{-1} and Met(O) approximately 226.5–230.3 kcal mol^{-1}, with very large uncertainties obtained when the Hunter and Lias scale and the Harrison scale were employed. The large uncertainty reported in Table 1 was the result of poor correlation in kinetic method plots (see Fig. 1 for kinetic method plots relative to the Hunter and Lias scale). More satisfactory results were obtained when the Tabet scale was employed, with lower uncertainties in the kinetic method plots (see Fig. 2). The improved fit of the

Table 1
Proton affinity of Met and Met(O) determined using both the simple and extended kinetic method using the *Hunter and Lias scale*, the *Harrison scale*, and the *Tabet scale* as the proton affinity of reference compounds

	PA (kcal mol^{-1})		
	Hunter and Lias	Harrison	Tabet
Simple kinetic method			
Met	221.6 ± 7.5	221.6 ± 3.6	221.5 ± 0.2
Met(O)	230.3 ± 3.9	229.8 ± 4.4	226.5 ± 0.7
Extended kinetic method			
Met	221.0 ± 0.2	223.1 ± 0.2	222.6 ± 0.2
Met(O)	234.0 ± 0.6	232.3 ± 0.5	227.5 ± 0.2

Collision energy used = 10 V (laboratory scale).

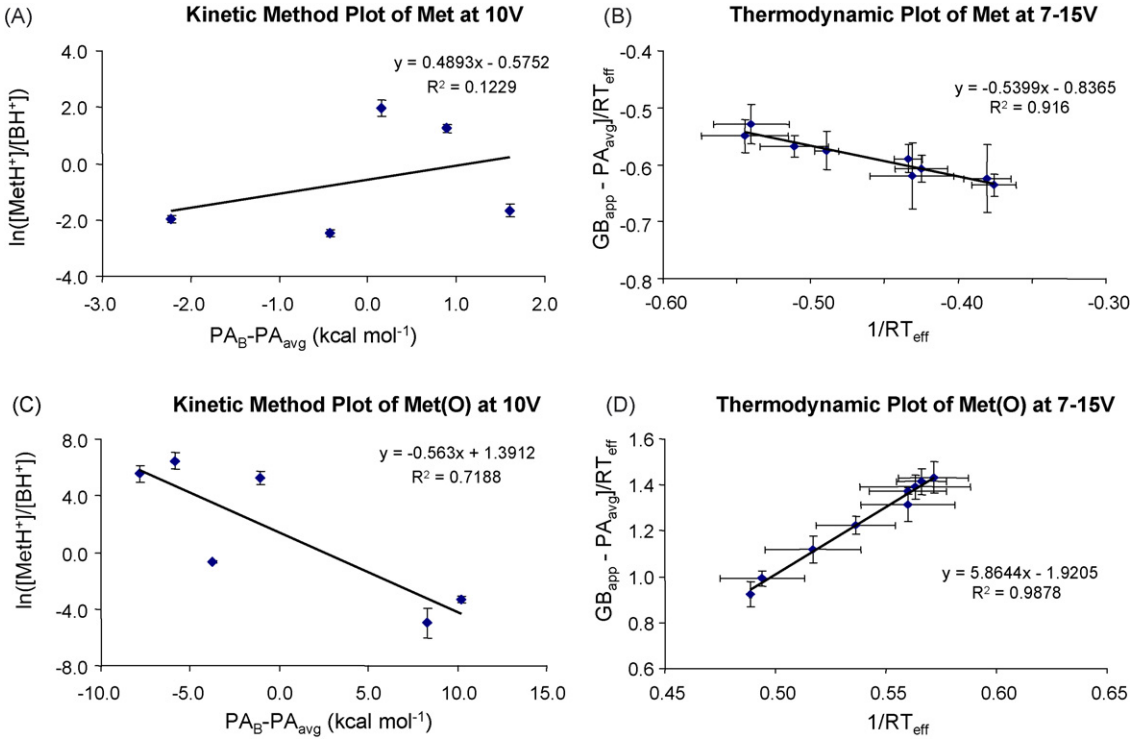

Fig. 1. Kinetic and thermodynamic plots of Met and Met(O) using the Hunter and Lias scale. (A) Typical kinetic method plot of Met at 10 V (laboratory scale), (B) thermodynamic plot of Met at 7–15 V (laboratory scale), (C) typical kinetic method plot of Met(O) at 10 V (laboratory scale), and (D) thermodynamic plot of Met(O) at 7–15 V (laboratory scale). Error bars are 95% confidence limits for three independent experiments. The reference bases used for Met were Pro, Asn, Glu, Tyr, and Phe; and for Met(O) were Asn, Trp, Pro, Gln, Lys, and His.

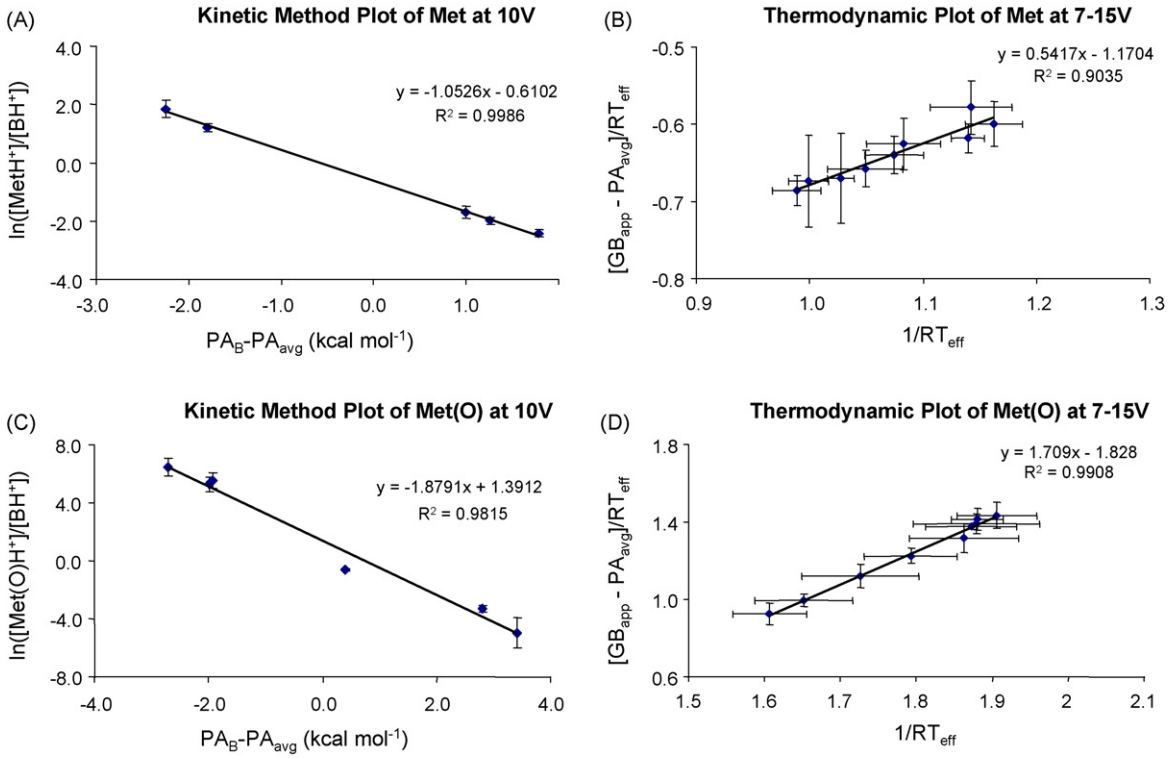

Fig. 2. Kinetic and thermodynamic plots of Met and Met(O) using the Tabet scale. (A) Typical kinetic method plot of Met at 10 V (laboratory scale), (B) thermodynamic plot of Met at 7–15 V (laboratory scale), (C) typical kinetic method plot of Met(O) at 10 V (laboratory scale), and (D) thermodynamic plot of Met(O) at 7–15 V (laboratory scale). Error bars are 95% confidence limits for three independent experiments. The reference bases used for Met were Pro, Asn, Glu, Tyr, and Phe; and for Met(O) were Asn, Trp, Pro, Gln, Lys, and His.

kinetic plots suggest that the Tabet scale is probably more accurate than the Hunter and Lias scale with respect to the order of basicity of amino acids in this proton affinity range. Since more precise results were obtained using the Tabet scale, the proton affinity of Met and Met(O) derivatives shall henceforth be given relative to the Tabet scale.

Using the extended kinetic method, the proton affinity of Met and Met(O) were determined to be 222.6 and 227.5 kcal mol^{-1}, respectively, relative to the Tabet scale. As one would expect, the kinetic method data from our experiments on Met are in good accord with Tabet's value for Met (221.7 kcal mol^{-1}). The data also clearly show that the proton affinity of Met(O) is much higher than Met (by about 5 kcal mol^{-1}).

3.2. DFT and ab initio calculations on the proton affinity of methionine and methionine sulfoxide

Fig. 3 shows the global minima of neutral and protonated Met and Met(O) obtained at the MP2/6-311 + G(2d,p)//B3LYP/6-31 + G(d,p) level of theory. The lowest energy conformer of *neutral* Met is stabilized by a hydrogen bond interaction between the amino and carbonyl groups, $NH_2 \rightarrow O{=}C$, which is further reinforced by additional $OH \rightarrow O{=}C$ interaction of *syn*-configuration of the carboxylic acid group. The global minimum of *protonated* Met (structure AH) is protonated at the amino group (the most basic site), and is stabilized by charge complexation by the side-chain sulfide group and the carbonyl group, $S \leftarrow NH_3^+ \rightarrow O{=}C$. The theoretical proton affinity of Met was predicted to be 224.0 kcal mol^{-1} at the MP2/6-311 + G(2d,p)//B3LYP/6-31 + G(d,p) level of theory (Table 2), somewhat higher than the experimental result. This is a general trend in the data, so we will focus mainly on values relative to Met rather than absolute values for comparison.

For Met(O), the most stable *neutral* species is stabilized by intramolecular hydrogen bonding involving the amino and carbonyl groups, $NH_2 \rightarrow O{=}C$, and further stabilized by strong hydrogen bonding interaction between the hydroxyl and sulfoxide groups, $OH \rightarrow O{=}S$. The latter interaction involves the less preferred *anti*-configuration of the carboxylic acid to enable stronger hydrogen bonding interaction with the side-chain (structure B). Amino protonated Met(O) is stabilized by charge complexation by both sulfoxide and carbonyl groups, $S{=}O \leftarrow NH_3^+ \rightarrow O{=}C$ (structure BH), in a similar fashion to that of Met. However, the increase in ring size involved in charge complexation (7-membered ring in Met(O)H$^+$ versus 6-membered ring in MetH$^+$) can contribute to forming a stronger hydrogen bond, and thus this stabilizes the proton more tightly [11]. It is noteworthy that the proton in protonated Met(O) appears to be equally hydrogen bonded by the amino and sulfoxide groups due to strong ionic hydrogen bond by sulfoxide group (see bond distances in structure BH). This results in

Table 2
Summary of experimental and theoretical proton affinity of methionine and methionine sulfoxide derivatives

Compound	Proton affinity (kcal mol^{-1})	
	Experimental[a]	Theoretical[b]
Met	221.5 ± 0.2[c] (0)	224.0 (0)
Met-OMe	224.9 ± 3.1 (3.4)	226.0 (2.0)
Met-NHMe	225.2 ± 0.6 (3.7)	228.3 (4.3)
Ac-Met	217.4 ± 0.4 (−4.1)	221.2 (−2.8)
Ac-Met-OMe	220.1 ± 0.4[d] (−1.4)	221.3 (−2.7)
Ac-Met-NHMe	224.1 ± 0.8 (2.6)	222.7 (−1.3)
Met(O)	226.5 ± 0.7[e] (5.0)	229.3 (5.3)
Met(O)-OMe	228.7 ± 1.3 (7.2)	235.1 (11.1)
Met(O)-NHMe	229.5 ± 2.4 (8.0)	235.0 (11.0)
Ac-Met(O)	224.3 ± 0.2 (2.8)	225.2 (1.2)
Ac-Met(O)-OMe	226.3 ± 1.2 (4.8)	230.5 (5.5)
Ac-Met(O)-NHMe	226.4 ± 1.6 (4.9)	227.6 (3.6)

[a] Determined using the simple kinetic method using the *Tabet scale* of amino acid proton affinities. The values shall be referred to as apparent proton affinities because no entropy corrections were made. Values relative to Met are given parenthetically. The listed uncertainties are a measure of error in the kinetic method approach and are best viewed as estimates of the relative uncertainties of the proton affinities. Superimposed on these are the 2–3 kcal mol^{-1} absolute uncertainties expected for the reference compounds.

[b] Calculated using MP2/6-311 + G(2d,p)//B3LYP/6-31 + G(d,p) level of theory. Values relative to Met are given parenthetically.

[c] Reported proton affinities are 221.7 kcal mol^{-1} [35], 223.6 kcal mol^{-1} [31], and 224.1 kcal mol^{-1} [32].

[d] Reported proton affinity is 224.5 kcal mol^{-1} [11].

[e] Reported theoretical proton affinity is 241.2 kcal mol^{-1} at the HF/6-31G(d) level of theory [45].

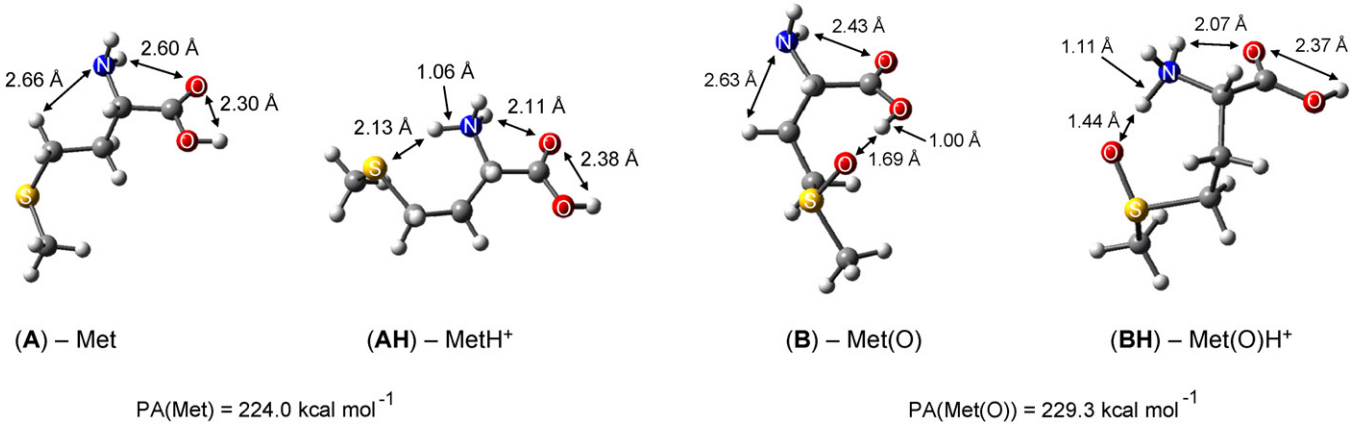

Fig. 3. B3LYP/6-31 + G(d,p) optimized structures of Met (A), MetH$^+$ (AH), Met(O) (B), and Met(O)H$^+$ (BH). Theoretical proton affinities of Met and Met(O) calculated at MP2/6-311 + G(2d,p)//B3LYP/6-31 + G(d,p) are 224.0 and 229.3 kcal mol^{-1}, respectively.

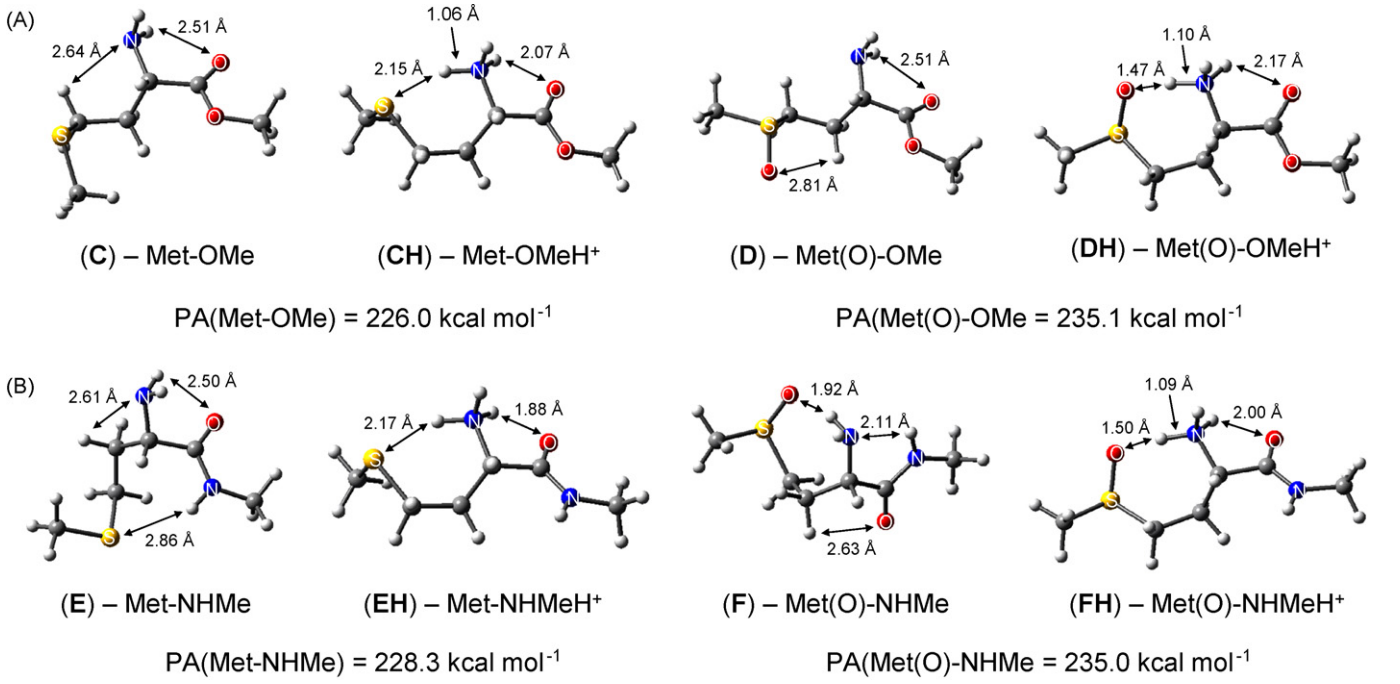

Fig. 4. (A) B3LYP/6-31 + G(d,p) optimized structures of Met-OMe (C), Met-OMeH$^+$ (CH), Met(O)-OMe (D), and Met(O)-OMeH$^+$ (DH); (B) B3LYP/6-31 + G(d,p) optimized structures of Met-NHMe (E), Met-NHMeH$^+$ (EH), Met(O)-NHMe (F), and Met(O)-NHMeH$^+$ (FH). Theoretical proton affinities of Met-OMe, Met(O)-OMe, Met-NHMe and Met(O)-NHMe calculated at MP2/6-311 + G(2d,p)//B3LYP/6-31 + G(d,p) are 226.0, 235.1, 228.3 and 235.0 kcal mol^{-1}, respectively.

a higher proton affinity of Met(O) than Met. At the MP2/6-311 + G(2d,p)//B3LYP/6-31 + G(d,p) level of theory, the proton affinity of Met(O) was predicted to be 229.3 kcal mol^{-1}, higher than the experimental value of 226.5 kcal mol^{-1}. However, the relative proton affinity of Met and Met(O) is computationally reproduced in excellent agreement (ΔPA = 5.0 kcal mol^{-1} versus 5.3 kcal mol^{-1} compared to Met). It is noteworthy that even though the neutral conformation calculated for Met(O) is stabilized by the presence of strong OH → O=S hydrogen bond, it may not be formed during the dissociation process (it requires conversion of a syn- to anti-conformation for the carboxylic acid group) and therefore a less stable neutral product might be formed in the experiments. If the most stable neutral Met(O) conformer without this hydrogen bond is used to calculate the proton affinity instead, the computed PA of Met(O) would be higher (see below).

3.3. Experimental and calculated proton affinities of C-terminally modified derivatives

3.3.1. Met-OMe and Met(O)-OMe

Table 2 lists the experimental and theoretical proton affinity of all the methionine and methionine sulfoxide derivatives studied. The proton affinity of Met-OMe was experimentally determined to be 224.9 kcal mol^{-1}, and the theoretical proton affinity is in good agreement with the experimental value. Both values are higher than the experimental and theoretical proton affinity predicted for Met (see Table 2). The lowest energy conformer of *protonated* Met-OMe is characterized by protonation at the amino group, which is stabilized by ionic hydrogen bonding involving both the sulfide group of the side-chain and the carbonyl group, S ← NH_3^+ → O=C (structure CH of Fig. 4). Since the methyl ester moiety is capable of forming a stronger hydrogen bond than the carboxylic acid (ionic hydrogen bond strength, $\Delta_r H^0$ (Eq. (11)) of methyl acetate = 29.1 kcal mol^{-1} and $\Delta_r H^0$ of acetic acid = 28.1 kcal mol^{-1} [50]), it is expected that Met-OMe is able to stabilize the proton to a greater extent than Met, resulting in a higher proton affinity.

$$BH^+ + B \rightarrow BHB^+ \quad (11)$$

Similarly, Met(O)-OMe has a higher proton affinity than Met(O) with an experimental proton affinity of 228.7 kcal mol^{-1}, 7.2 kcal mol^{-1} greater than Met. The theoretical proton affinity of Met(O)-OMe is predicted to be much higher (235.1 kcal mol^{-1}) and only modest agreement is seen in the computed value relative to Met (ΔPA = 11.1 kcal mol^{-1}). The B3LYP/6-31 + G(d,p) optimized structures for the global minima of neutral and protonated Met(O)-OMe are shown as structures D and DH, respectively, in Fig. 4(A). The structure of *protonated* Met(O)-OMe is very similar to Met(O) in terms of the site of proton attachment and its stabilization (compare structure DH with structure BH). The lowest energy conformer of *protonated* Met(O)-OMe is protonated at the amino group, which is charge complexed by both the sulfoxide and carbonyl groups, S=O ← NH_3^+ → O=C (see structure DH). Similar to protonated Met(O), the proton is equally hydrogen bonded by the amino and sulfoxide groups. This charge complexation of Met(O)-OMe by the side-chain sulfoxide group (S=O) involves the formation of a 7-membered ring. As with Met and Met(O), the stronger hydrogen bonding capability of the sulfoxide group leads to a higher proton affinity for Met(O)-OMe compared to Met-OMe. The large difference in computed proton affinities

between Met(O) and Met(O)-OMe is caused mainly by differences in the neutrals because the structures of the protonated forms are nearly identical and the added methyl group should not increase the PA by 6 kcal mol^{-1} (only a 2 kcal mol^{-1} difference is seen between Met and Met-OMe). The ability of Met(O) to form a strong OH → O=S hydrogen bond, which is impossible for Met(O)-OMe, causes significant stabilization of the neutral form and thus reduces its computed PA. This leads to the large difference in the computed PA's of Met(O) and Met(O)-OMe. Because this difference in PA's is not seen experimentally, it is very possible that the conformation with the OH → O=S interaction is not accessible in the CID experiments. If the one uses a Met(O) conformation lacking this interaction for the PA calculation, the Met(O)/Met(O)-OMe PA difference is close to the experimental value. It is true that the computed PA for Met(O) is closer to the measured one, this does guarantee that it is more accurate because the data suggest that the computed values may be systematically high for Met(O) derivatives.

3.3.2. Met-NHMe and Met(O)-NHMe

The experimental proton affinity of Met-NHMe was determined to be 225.2 kcal mol^{-1}, slightly higher than that of Met-OMe and 3.7 kcal mol^{-1} higher than Met (Table 2). This is consistent with the higher ionic hydrogen bond strength ($\Delta_r H^0$ (of reaction (11)) of methyl acetamide (29.8 kcal mol^{-1}) compared to methyl acetate (29.1 kcal mol^{-1}) [50]. The most stable conformers of the neutral and protonated species of Met-NHMe optimized at the B3LYP/6-31 + G(d,p) level of theory are shown in Fig. 4(B) (structures E and EH, respectively). The global minimum of *neutral* Met-NHMe (structure E) has very similar interactions to *neutral* Met-OMe (structure C), except for additional NH → S hydrogen bond in Met-NHMe. Interestingly, this amide N–H does not participate in hydrogen bonding of the *protonated* species. The theoretical proton affinity of Met-NHMe was predicted to be 4.3 kcal mol^{-1} higher than Met.

The proton affinity of Met(O)-NHMe was experimentally determined to be 229.5 kcal mol^{-1}, a proton affinity value that is close to that of Met(O)-OMe and 8 kcal mol^{-1} greater than Met. Close examination of the predicted neutral and protonated Met(O)-NHMe structures (structures F and FH in Fig. 4(B)) reveals that differences in intramolecular bonding in *both* the neutral and protonated species may explain the similar proton affinities of Met(O)-NHMe and Met(O)-OMe. Strong stabilization of the *neutral* Met(O)-NHMe species by multiple intramolecular hydrogen bonding would decrease the proton affinity, while strong stabilization of the *protonated* Met(O)-NHMe species by the C-terminal amide group would increase the proton affinity of the molecule. The global minimum of *neutral* Met(O)-NHMe (structure F in Fig. 4(B)) is highly stabilized by intramolecular hydrogen bonding interaction between the C-terminal amide group and the amino group, and by a further cooperative hydrogen bond interaction [51] with the sulfoxide group, C(O)NH → NH_2 → O=S (structure F). This multiple hydrogen bonding in Met(O)-NHMe is enabled by the presence of the amide N–H. The global minimum of *protonated* Met(O)-NHMe (structure FH) has very similar features to that of Met(O)-OMe. The proton is attached to the most basic functional group, the amino group, and is stabilized by charge complexation involving hydrogen bonding interaction with the side-chain sulfoxide group as well as the carbonyl group, S=O ← NH_3^+ → O=C. Interestingly, the C-terminal amide N–H does not participate in any hydrogen bonding interaction. Together, the overall effect of these stabilization interactions in both the neutral and protonated structures are expected to result in the proton affinity of Met(O)-NHMe being similar to that of Met(O)-OMe. The theoretical proton affinity of Met(O)-NHMe was predicted to be 11 kcal mol^{-1} greater than Met.

3.4. Experimental and calculated proton affinities of N-terminally modified derivatives

3.4.1. Ac-Met and Ac-Met(O)

Ac-Met was determined using the extended kinetic method to have a proton affinity value of 217.4 kcal mol^{-1} (Table 2), lower than that of Met (221.5 kcal mol^{-1}). Since the amino group is blocked by an *N*-acetyl group, the decrease in proton affinity is due to a change in the site of protonation as well as differences in charge stabilization. The calculated lowest energy conformers of neutral and protonated Ac-Met are shown as structures G and GH, respectively, in Fig. 5. The predicted site of protonation in Ac-Met is the carbonyl oxygen of the *N*-acetyl group, stabilized by ionic hydrogen bonding with the sulfide group of the side-chain, C=OH^+ → S (structure GH of Fig. 5). Further stabilization is provided by charge delocalization via a protonated imine resonance structure (Scheme 1). The proton is only stabilized by one functional group (structure GH), which results in a weaker stabilization of the charge in Ac-Met compared to Met, and hence a lower proton affinity. The theoretical proton affinity of Ac-Met was calculated to be 2.8 kcal mol^{-1} lower than Met.

Both the experimental and theoretical proton affinities for Ac-Met(O) are lower than that of the unmodified Met(O) (the experimentally determined proton affinity of Ac-Met(O) was 224.3 kcal mol^{-1} compared to 226.5 kcal mol^{-1} for Met(O)). As with the case of Ac-Met, this can be rationalized in terms of changes in the site of protonation and different types of charge stabilization. Fig. 5 shows the global minima predicted for neutral and protonated Ac-Met(O) (structures H and HH, respectively). It is noteworthy that *neutral* Ac-Met(O) is stabilized by two intramolecular hydrogen bonds involving the *N*-acetyl amide group. The energetically unfavorable anti-configuration of carboxylic acid interacts with the amide carbonyl, OH → O=C, in a similar fashion to *neutral* Met(O), and the amide N–H group interacts with the side-chain sulfoxide group, C(O)NH → O=S (structure H).

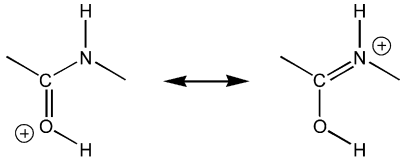

Scheme 1.

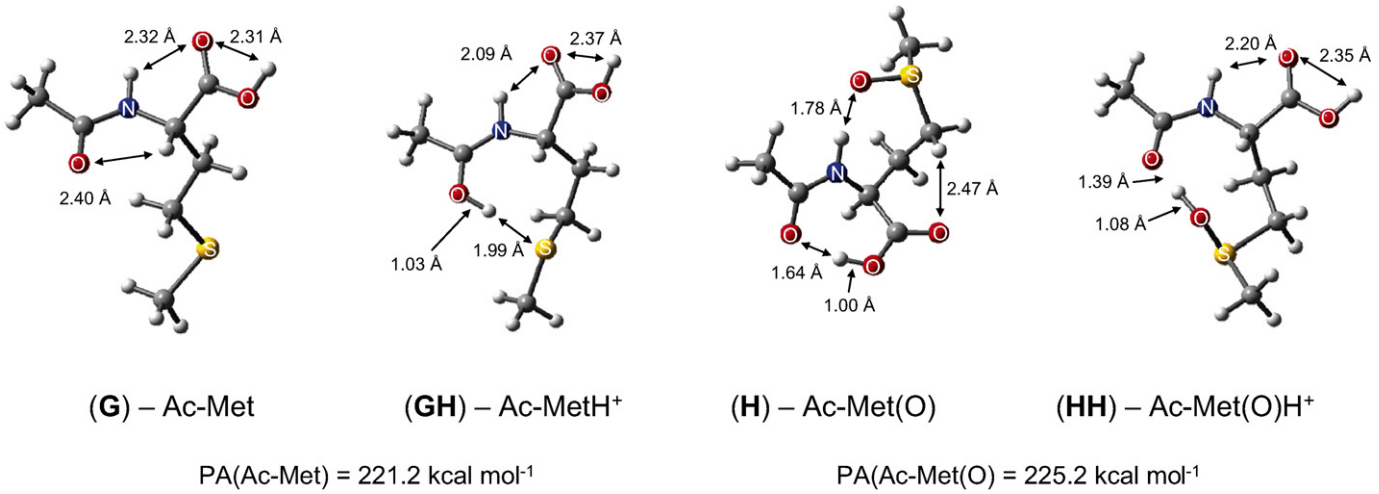

Fig. 5. B3LYP/6-31 + G(d,p) optimized structures of Ac-Met (G), Ac-MetH$^+$ (GH), Ac-Met(O) (H), and Ac-Met(O)H$^+$ (HH). Theoretical proton affinities of Ac-Met and Ac-Met(O) calculated at MP2/6-311 + G(2d,p)//B3LYP/6-31 + G(d,p) are 221.2 and 225.2 kcal mol^{-1}, respectively.

The site of proton attachment in Ac-Met(O) was predicted to be the sulfoxide group of the side-chain, stabilized by a strong ionic hydrogen bond to the *N*-acetyl carbonyl group, S=OH$^+$ → O=C, via the formation of a 9-membered ring (structure HH of Fig. 5). The proton can be seen as being equally hydrogen bonded by the *N*-acetyl carbonyl and sulfoxide groups. Similar to Ac-Met, the attached proton is stabilized only by one functional group, resulting in a lower proton affinity for Ac-Met(O) compared to Met(O). The theoretical proton affinity of Ac-Met(O) was predicted to be 1.2 kcal mol^{-1} higher than Met, similar to the experimental value, which is 2.8 kcal mol^{-1} greater then Met. In a similar way to unusually stable neutral Met(O) described above, the strong hydrogen bond (OH → O=S) in neutral Ac-Met(O) leads to a low computed PA, but it is unlikely that this species is accessed in the dissociation experiments. If the experimental data is based on the formation of an Ac-Met(O) neutral conformation without this hydrogen bond, a PA higher than the computational one would be observed (see Section 4.2).

3.5. Experimental and DFT calculated proton affinities of N- and C-terminally modified derivatives

3.5.1. Ac-Met-OMe and Ac-Met(O)-OMe

The proton affinity of Ac-Met-OMe was determined to be 220.1 kcal mol^{-1} using the simple kinetic method (Table 2). This value is higher than that of Ac-Met, but much lower than a previously determined proton affinity value of Ac-Met-OMe of 224.5 kcal mol^{-1} [11]. The difference is likely related to the choice of reference scales. As previously observed for the increase in proton affinity from Met to Met-OMe, the increase in proton affinity from Ac-Met to Ac-Met-OMe may be due to the enhanced capacity of a methyl ester to stabilize the proton.

The structures of the global minima found for *neutral* and *protonated* Ac-Met-OMe optimized at the MP2/6-311 + G(2d,p)//B3LYP/6-31 + G(d,p) level of theory are shown as structures I and IH, respectively, in Fig. 6(A). The global minimum of protonated Ac-Met-OMe (structure IH of Fig. 6(A)) is characterized by protonation at the *N*-acetyl carbonyl group, which is stabilized by intramolecular ionic hydrogen bond to the C-terminal carbonyl group, C=OH$^+$ → O=C, as well as a hydrogen bond between *N*-acetyl amide and side-chain sulfide, C(O)NH → S. Stabilization of protonated Ac-Met-OMe is further aided by charge delocalization to form the protonated imine resonance structure (Scheme 1). The theoretical proton affinity of Ac-Met-OMe was predicted to be 221.3 kcal mol^{-1}, in reasonable agreement with the experimental value.

The experimentally determined proton affinity of Ac-Met(O)-OMe was found to be 226.3 kcal mol^{-1} (Table 2). As anticipated from the other methionine and methionine sulfoxide derivatives, this proton affinity value is higher than both Ac-Met(O) and Ac-Met-OMe due to differences in charge stabilization capability. The global minima structures of neutral and protonated Ac-Met(O)-OMe optimized at the B3LYP/6-31 + G(d,p) level of theory are shown as structures J and JH, respectively, in Fig. 6(A). Interestingly, the bonding interactions present in *neutral* Ac-Met(O)-OMe and the site of protonation and geometry of *protonated* Ac-Met(O)-OMe closely resemble those of Ac-Met(O) (structures H and HH) The theoretical proton affinity of Ac-Met(O)-OMe was predicted to be 230.5 kcal mol^{-1}.

3.5.2. Ac-Met-NHMe and Ac-Met(O)-NHMe

From Table 2, it can be seen that the proton affinity of Ac-Met-NHMe was experimentally determined to be 224.1 kcal mol^{-1}, higher than that of both Ac-Met and Ac-Met-OMe. Fig. 6(B) shows the global minimum structures of neutral and protonated Ac-Met-NHMe. The intramolecular stabilization of *neutral* Ac-Met-NHMe is very similar to that of Ac-Met-OMe (structure I), except for an additional hydrogen bond due to the presence of the C-terminal amide N–H in Ac-Met-NHMe. On the other hand *protonated* Ac-Met-NHMe does not involve the C-terminal amide group in any stabilization process, closely resembling the methyl ester counterparts (structure IH). The theoretical proton affinity of Ac-Met-NHMe was predicted to be 222.7 kcal mol^{-1}, or 1.3 kcal mol^{-1} less than Met. In contrast, the experimen-

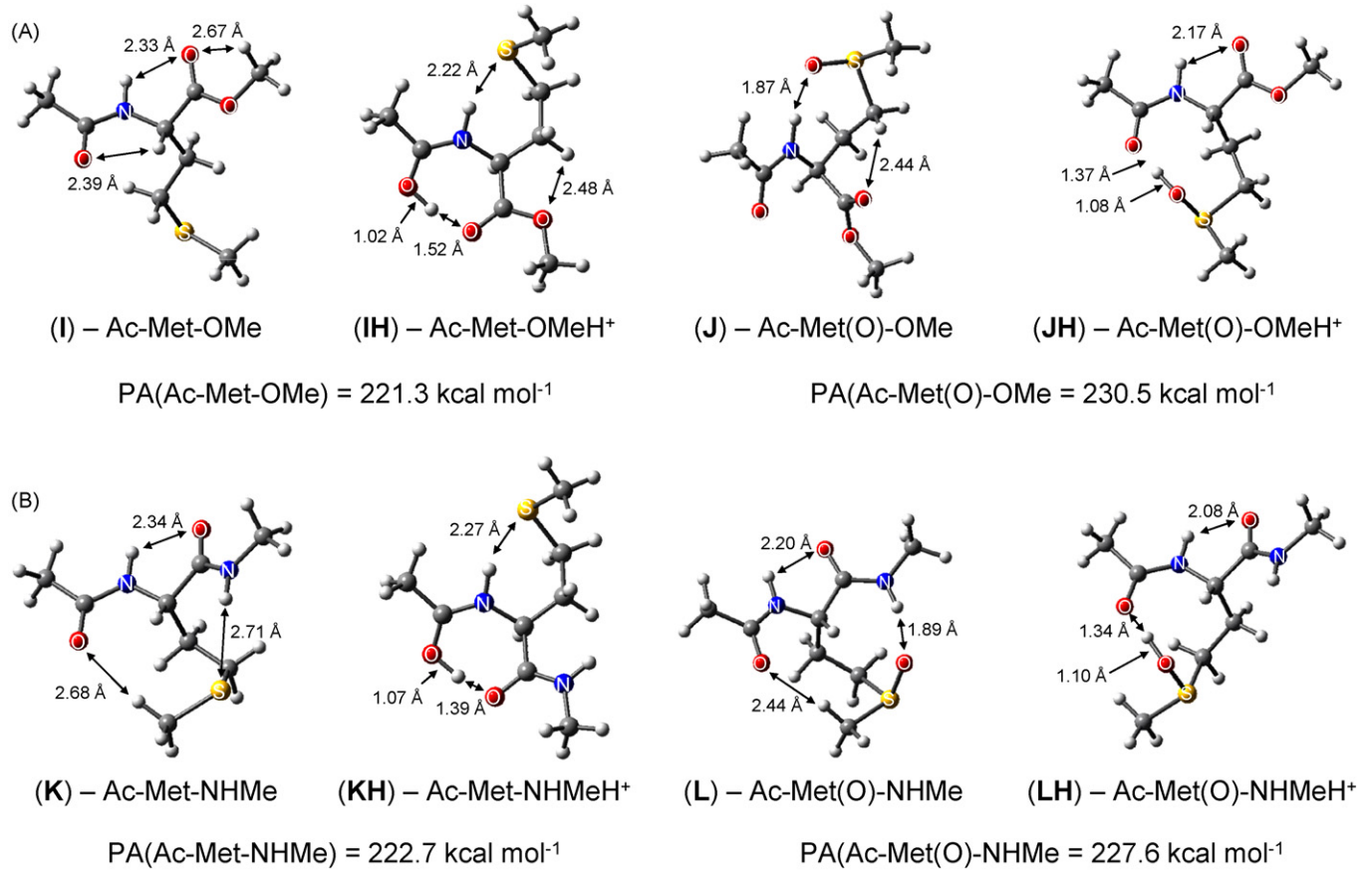

Fig. 6. (A) B3LYP/6-31 + G(d,p) optimized structures of Ac-Met-OMe (I), Ac-Met-OMeH$^+$ (IH), Ac-Met(O)-OMe (J), and Ac-Met(O)-OMeH + (JH); (B) B3LYP/6-31 + G(d,p) optimized structures of Ac-Met-NHMe (K), Ac-Met-NHMeH + (KH), Ac-Met(O)-NHMe (L), and Ac-Met(O)-NHMeH + (LH). Theoretical proton affinities of Ac-Met-OMe, Ac-Met(O)-OMe, Ac-Met-NHMe and Ac-Met(O)-NHMe calculated at MP2/6-311 + G(2d,p)//B3LYP/6-31 + G(d,p) are 221.3, 230.5, 222.7 and 227.6 kcal mol^{-1}, respectively.

tal value suggests a higher PA for Ac-Met-NHMe than Met. However, the theoretical proton affinity of Ac-Met-NHMe is in agreement with the experimental results in that this value is higher than the theoretical proton affinity of both Ac-Met and Ac-Met-OMe (see Table 2). Like Met(O), the difference between the computed and experimental PA's for Ac-Met-NHMe may be related to extensive hydrogen bonding in the computed conformation of neutral Ac-Met-NHMe. If dissociation leads to a looser, but less stable neutral conformation for Ac-Met-NHMe, the experimental PA would appear to be larger than the computed one. A key point is that the experiments are accessing the species with the lowest free energy whereas the calculations are targeting the species with the lowest enthalpy. This issue is considered in greater detail in Section 4.

The proton affinity of Ac-Met(O)-NHMe was experimentally determined to be 226.4 kcal mol^{-1} (Table 2). This value gives Ac-Met(O)-NHMe a higher proton affinity than Ac-Met-NHMe, but interestingly, the same proton affinity value with Ac-Met(O)-OMe. The higher proton affinity of Ac-Met(O)-NHMe than Ac-Met-NHMe is due to the enhanced capacity of the sulfoxide group to stabilize the ionizing proton. The global minimum of the *neutral* and *protonated* Ac-Met(O)-NHMe structures are shown in Fig. 6(B) as structures L and LH, respectively. Overall, the structures of *neutral* and *protonated* Ac-Met(O)-NHMe have very similar bonding interactions to Ac-Met(O)-OMe. The theoretical proton affinity of Ac-Met(O)-NHMe was predicted to be 227.6 kcal mol^{-1} at the MP2/6-311 + G(2d,p)//B3LYP/6-31 + G(d,p) level of theory. This value is lower than the theoretical proton affinity of Ac-Met(O)-OMe (230.5 kcal mol^{-1}) and reflects the unusually strong hydrogen bonding interactions that stabilize the *neutral* Ac-Met(O)-NHMe. As with Ac-Met-NHMe, the computed, neutral Ac-Met(O)-NHMe conformation has extensive, strong hydrogen bonding and may not match the conformation that is formed experimentally. This would explain the low PA computed for Ac-Met(O)-NHMe.

4. Discussion

From the results described above, it is clear that there is a general agreement between the experimental and theoretically predicted proton affinities, with some exceptions. These differences can be attributed to a number of sources. Experimentally, the result of kinetic factors (see below) could lead to some of the differences. The computational method could give poor energies for some bonding schemes or the chosen structures might not be true global minima. Although the conformational searches were relatively expansive, a lower energy structure may have been

missed. Nonetheless, the extensive hydrogen bonding observed in the computed structures suggests that they are highly stabilized and likely candidates for the global minima. Given the wide variety of bonding schemes in these complexes, it would not be surprising if the modest levels of theory used here were unable to characterize them all equally well. However, since the computational values are generally within the anticipated experimental uncertainties of the measurements, they provide useful structural insights into interpreting the trends in proton affinity.

4.1. Influence of amino acid modification on proton affinity

Table 2 summarizes the experimental and theoretical proton affinity of all the methionine and methionine sulfoxide derivatives studied. The influence of the methionine modifications on the proton affinities are discussed below.

4.1.1. Oxidation

Oxidation of methionine derivatives results in an increase in proton affinity in every case. This increase can be explained by a combination of two factors. Firstly, sulfoxide groups have intrinsically higher proton affinities than sulfide groups (PA(dimethyl sulfoxide) = 211.4 kcal mol^{-1} versus PA (dimethyl sulfide) = 198.6 kcal mol^{-1} [31]. The sulfoxide moiety also has stronger ionic hydrogen bonding than sulfide groups (ionic hydrogen bond strength, $\Delta_r H^0$ (of Eq. (11)) of dimethyl sulfoxide = 30.8 kcal mol^{-1} and $\Delta_r H^0$ of dimethyl sulfide = 26.4 kcal mol^{-1} [50]). The individual effect, or a combination of the above factors, suggests that the sulfoxide moiety has a greater capacity to stabilize a proton through charge complexation than the sulfide moiety. Secondly, the increase in ring size formed through charge complexation by the sulfoxide compared to the sulfide may allow more efficient hydrogen bonding [52–56]. This results in a higher proton affinity of the methionine sulfoxide derivatives.

4.1.2. Methyl esterification and methyl amidation

C-terminal modification of methionine, methionine sulfoxide and their derivatives by methyl esterification and methyl amidation increases the resultant proton affinity. These results are consistent with an increase in the charge stabilization capacity of methyl esters and methyl amides compared to carboxylic acids. In addition, the C-terminal modifications do not allow for the strong $CO_2H \rightarrow O{=}S$ hydrogen bonding observed in the calculations on some of the neutral Met(O) derivatives, a factor that increase their computed PA's.

4.1.3. N-Acetylation

The proton affinity of *N*-acetylated methionine and methionine sulfoxide is lower than their unmodified amino acids. This is due to a change in the site of protonation from the amino group to the *N*-acetyl carbonyl group for the unoxidized methionine derivative or to the side-chain sulfoxide group for the oxidized methionine derivative. Additionally, the proton that is attached to the *N*-acetyl carbonyl or side-chain sulfoxide is stabilized by only one functional group instead of two when it is protonated at the amino group. This weakens the charge stabilization and results in lower proton affinities for the *N*-acetylated derivatives.

4.1.4. A combination of modifications

Multiple combinations of N- and C-terminal methionine modifications are observed to affect the proton affinity in an additive fashion. For example, the proton affinity of Ac-Met(O)-OMe is close to that of Met(O) because of an increase in proton affinity due to methyl esterification which offsets the decrease in proton affinity due to *N*-acetylation.

4.2. Site of protonation

The various sites of protonation in methionine and methionine sulfoxide derivatives reveal an interesting trend. From Figs. 3 and 4, the site of protonation of the methionine and methionine sulfoxide derivatives with unmodified N-termini is the amino group, whereas Figs. 5 and 6 show that *N*-acetylated methionine and *N*-acetylated methionine sulfoxide derivatives are protonated at the *N*-acetyl carbonyl C=O and side-chain sulfoxide S=O, respectively. The trend observed is consistent with protonation occurring at the site that has the best ability to stabilize the acquired charge [55,57], which in this study corresponds to the site with the highest intrinsic proton affinity. Further stabilization can also be provided by delocalization of the acquired charge through intramolecular hydrogen bonding. When the difference in proton affinity between the functional group for the site of protonation and the site that stabilizes the proton is small (ΔPA is small), the proton is equally stabilized by hydrogen bonds to the two functional groups. In this work the preferred site of protonation is amino group > sulfoxide group > *N*-acetyl carbonyl group. The C-terminal methyl ester and carboxylic acid functional group are never protonated due to their low proton affinity.

4.3. Influence of intramolecular hydrogen bonding of neutral species on proton affinity

From Figs. 3–6, all protonated methionine and methionine sulfoxide derivatives are stabilized by intramolecular ionic hydrogen bonds. Cyclization of protonated bifunctional species by intramolecular ionic hydrogen bonding is known to cause an increase in their proton affinities [55]. A topic that has received less attention in the literature is the stabilization of neutral species, which also contributes to the overall proton affinity. McMahon and co-workers have studied the phenomena of neutral stabilization using a combination of equilibrium proton transfer reactions in a Fourier transform ion-cyclotron resonance mass spectrometry (FT-ICR MS) and theoretical calculations [58]. Their theoretical calculations of the neutral conformers of ω-methoxy alcohol at the MP2/6-31G(d)//HF/6-31G(d) level of theory suggested that the cyclic form is more stabilized by enthalpy. However, from equilibrium measurements in the FT-ICR, and by calculations of mean thermal energies of neutral ω-methoxy alcohol, it was argued that except for methoxyethanol, ω-methoxy alcohol primarily exists in linear form due to entropic effects.

We observe similar neutral stabilization by strong intramolecular hydrogen bonds in Met(O), Ac-Met(O), Ac-Met-NHMe, and Ac-Met(O)-NHMe (see structures B, H, K, and L, respectively). *Neutral* Met(O) and Ac-Met(O) (structures B and H) are stabilized by strong intramolecular hydrogen bond due to *anti*-configuration of the carboxylic acids, OH → O=C, whereas *neutral* Ac-Met-NHMe and Ac-Met(O)-NHMe (structures K and L, respectively) is stabilized by a network of hydrogen bonds that is made possible by the presence of N- and C-terminal amide groups. These favorable intramolecular hydrogen bonds are "replaced" when the derivatives are protonated. The overall effect is to reduce the resultant proton affinities. For example, Met(O) is calculated to be significantly less basic than Met(O)-OMe, not because protonated Met(O)-OMe is significantly more stabilized than Met(O), but because neutral Met(O) has more favorable interactions than neutral Met(O)-OMe. Thus, Met(O) does not benefit from extra stabilization upon protonation. *Protonated* Met(O) and Met(O)-OMe have very similar charge stabilization interactions (see structures BH and DH, respectively). Similarly, Ac-Met(O)-NHMe is calculated to be less basic than Ac-Met(O)-OMe due to stronger hydrogen bonding in the *neutral* Ac-Met(O)-NHMe. This result is inconsistent if the only effect taken into consideration is stabilization of protonated species by the C-terminal functional group.

This may also explain some of the differences observed between the experimental and theoretical proton affinities. During the dissociation of proton bound dimer, it seems unlikely that the neutral, departing amino acid will be able to adopt all the hydrogen bonding interactions that have been identified computationally for the lowest enthalpy structure. In particular, this would be problematic for species that prefer *syn*-carboxylic acid conformations in the cations and *anti*-carboxylic acid conformations in the neutral amino acids. Thus, a key uncertainty in the application of the kinetic method to highly functionalized molecules is whether dissociation from the dimer results in the preferred, 298 K conformation for all charged ($(MH)^+$ of Eq. (1) and $(BH)^+$ of Eq. (2)) and neutral (B of Eq. (1) and M of Eq. (2)) monomers.

5. Conclusions

The present study employs the kinetic method to experimentally determine the proton affinity of methionine, methionine sulfoxide and their derivatives using amino acids as the reference bases. In addition, DFT calculations were carried out to determine theoretical proton affinities as well as to provide structural insights into different types of stabilization of neutral and protonated species. Generally, the theoretical proton affinities are in reasonable agreement with the experimental results, with agreement being better for changes in proton affinity upon simple methionine modification. While a number of factors might contribute to discrepancies between the theoretical and experimental proton affinities, a key factor may be that while theoretical proton affinities use the calculated enthalpies of global minima of both the neutral and protonated species, dissociation of proton bound dimers during MS/MS experiments does not guarantee the formation of all monomeric species (protonated and neutral monomers in Eqs. (1) and (2)) in their most stable conformation. In particular, the DFT calculations reveal that a number of neutral species are stabilized by a network of intramolecular hydrogen bonds which differ to their protonated form, and these may not be accessed during the experiments.

This study highlights that a post-translational modification not only influences the local proton affinity of a residue, but can also change the initial site of protonation. Furthermore, simple modification of the N- and/or the C-terminus of amino acids can change the proton affinity significantly. For example, *N*-acetylation of methionine and methionine sulfoxide lowers their proton affinities. Interestingly, this difference appears to have consequences in the fragmentation efficiency curves of protonated *N*-acetylated peptides, which require lower collision energies than the unmodified peptides [4]. In contrast, peptide ions containing methionine sulfoxide residues are observed to fragment at higher energies than the same peptide containing an unoxidized methionine [10]. This observation may be rationalized from the proton affinity measurements presented here in terms of the proton being "less mobile" in the case of the methionine sulfoxide containing peptides. Thus, the higher local proton affinity of the oxidized residue requires more energy to "mobilize" the proton to other sites for fragmentation. Studies on the fragmentation energetics and dynamics of methionine sulfoxide containing peptides using time and energy resolved surface induced dissociation are underway and will be presented elsewhere.

Acknowledgments

R.A.J.O. thanks the Australian Research Council (ARC) for financial support. H.L. acknowledges the award of an Elizabeth and Vernon Puzey Postgraduate Research Scholarship and John and Allan Gilmour Scholarship. S.G. acknowledges support from the National Science Foundation (CHE-0348809). G.E.R. acknowledges support from a National Science Foundation CAREER award (CHE 0547940). We gratefully acknowledge support for this work from the Ludwig Institute for Cancer Research and the Victorian Institute for Chemical Sciences High Performance Computing Facility.

Appendix A. Supplementary data

The following are available from the authors upon request:

(1) complete data of reference bases used for each methionine and methionine sulfoxide derivatives studied,
(2) dissociation data consisting of logarithmic ratio of ion abundance for each methionine and methionine sulfoxide derivatives studied, and
(3) complete structural details for each of the B3LYP/6-31 + G** optimized structures.

Supplementary data associated with this article can be found, in the online version, at doi:10.1016/j.ijms.2007.02.038.

References

[1] K.M. Ervin, Chem. Rev. 101 (2001) 391.
[2] K. Breuker, R. Knochenmuss, J. Zhang, A. Stortelder, R. Zenobi, Int. J. Mass Spectrom. 226 (2003) 211.
[3] E.A. Kapp, F. Schuetz, G.E. Reid, J.S. Eddes, R.L. Moritz, R.A.J. O'Hair, T.P. Speed, R.J. Simpson, Anal. Chem. 75 (2003) 6251.
[4] A.R. Dongre, J.L. Jones, A. Somogyi, V.H. Wysocki, J. Am. Chem. Soc. 118 (1996) 8365.
[5] R.A.J. O'Hair, J. Mass Spectrom. 35 (2000) 1377.
[6] G. Tsaprailis, H. Nair, A. Somogyi, V.H. Wysocki, W. Zhong, J.H. Futrell, S.G. Summerfield, S.J. Gaskell, J. Am. Chem. Soc. 121 (1999) 5142.
[7] D.G. Morgan, M.M. Bursey, Org. Mass Spectrom. 29 (1994) 354.
[8] D.G. Morgan, M.M. Bursey, J. Mass Spectrom. 30 (1995) 290.
[9] R.A.J. O'Hair, G.E. Reid, Eur. J. Mass Spectrom. 5 (1999) 325.
[10] G.E. Reid, K.D. Roberts, E.A. Kapp, R.J. Simpson, J. Proteome Res. 3 (2004) 751.
[11] V. Addario, Y. Guo, I.K. Chu, Y. Ling, G. Ruggerio, C.F. Rodriquez, A.C. Hopkinson, K.W.M. Siu, Int. J. Mass Spectrom. 219 (2002) 101.
[12] R.D. Kinser, G. Nicol, D.P. Ridge, J. Phys. Chem. A 106 (2002) 9925.
[13] A.A. Bliznyuk, H.F. Schaefer III, I.J. Amster, J. Am. Chem. Soc. 115 (1993) 5149.
[14] R.W. Feenstra, E.H.M. Stokkingreef, A.M. Reichwein, W.B.H. Lousberg, H.C.J. Ottenheijm, Tetrahedron 46 (1990) 1745.
[15] R.G. Cooks, J.T. Koskinen, P.D. Thomas, J. Mass Spectrom. 34 (1999) 85.
[16] S.A. McLuckey, D. Cameron, R.G. Cooks, J. Am. Chem. Soc. 103 (1981) 1313.
[17] R.G. Cooks, P.S.H. Wong, Acc. Chem. Res. 31 (1998) 379.
[18] R.G. Cooks, T.L. Kruger, J. Am. Chem. Soc. 99 (1977) 1279.
[19] L. Drahos, K. Vekey, J. Mass Spectrom. 34 (1999) 79.
[20] K.M. Ervin, Int. J. Mass Spectrom. 195–196 (2000) 271.
[21] Z. Wu, C. Fenselau, Rapid Commun. Mass Spectrom. 8 (1994) 777.
[22] Z. Wu, C. Fenselau, Tetrahedron 49 (1993) 9197.
[23] B.A. Cerda, C. Wesdemiotis, J. Am. Chem. Soc. 118 (1996) 11884.
[24] B.A. Cerda, S. Hoyau, G. Ohanessian, C. Wesdemiotis, J. Am. Chem. Soc. 120 (1998) 2437.
[25] M.J. Nold, B.A. Cerda, C. Wesdemiotis, J. Am. Soc. Mass Spectrom. 10 (1999) 1.
[26] P.B. Armentrout, J. Am. Soc. Mass Spectrom. 11 (2000) 371.
[27] K.M. Ervin, J. Am. Soc. Mass Spectrom. 13 (2002) 435.
[28] G.S. Gorman, J.P. Speir, C.A. Turner, I.J. Amster, J. Am. Chem. Soc. 114 (1992) 3986.
[29] M. Meot-Ner, E.P. Hunter, F.H. Field, J. Am. Chem. Soc. 101 (1979) 686.
[30] S.G. Lias, J.F. Liebman, R.D. Levin, J. Phys. Chem. Ref. Data 13 (1984) 695.
[31] E.P. Hunter, S.G. Lias, in: P.J. Linstrom, W.G. Mallard (Eds.), NIST Chemistry WebBook, NIST Standard Reference Database Number 69, National Institute of Standards and Technology, Gaithersburg, MD 20899, June 2005, http://webbook.nist.gov.
[32] A.G. Harrison, Mass Spectrom. Rev. 16 (1997) 201.
[33] G. Bojesen, T. Breindahl, J. Chem. Soc., Perkin Trans. 2 (1994) 1029.
[34] X. Li, A.G. Harrison, Org. Mass Spectrom. 28 (1993) 366.
[35] C. Afonso, F. Modeste, P. Breton, F. Fournier, J.C. Tabet, Eur. J. Mass Spectrom. 6 (2000) 443.
[36] Z.B. Maksic, B. Kovacevic, Chem. Phys. Lett. 307 (1999) 497.
[37] C. Bleiholder, S. Suhai, B. Paizs, J. Am. Soc. Mass Spectrom. 17 (2006) 1275.
[38] S.P. Mirza, S. Prabhakar, M. Vairamani, Rapid Commun. Mass Spectrom. 15 (2001) 957.
[39] A.F. Kuntz, A.W. Boynton, G.A. David, K.E. Colyer, J.C. Poutsma, J. Am. Soc. Mass Spectrom. 13 (2002) 72.
[40] O.E. Schroeder, E.J. Andriole, K.L. Carver, K.E. Colyer, J.C. Poutsma, J. Phys. Chem. A 108 (2004) 326.
[41] S. Mezzache, C. Afonso, C. Pepe, P. Karoyan, F. Fournier, J.C. Tabet, Rapid Commun. Mass Spectrom. 17 (2003) 1626.
[42] C. Pepe, S. Rochut, J.P. Paumard, J.C. Tabet, Rapid Commun. Mass Spectrom. 18 (2004) 307.
[43] T. Marino, N. Russo, E. Tocci, M. Toscano, J. Mass Spectrom. 36 (2001) 301.
[44] M. Noguera, L. Rodriguez-Santiago, M. Sodupe, J. Bertran, Theochem 537 (2001) 307.
[45] Y.A. Borisov, Y.A. Zolotarev, E.V. Laskatelev, N.F. Myasoedov, Russ. Chem. Bull. 47 (1998) 1442.
[46] W.J. Hehre, J.A. Pople, L. Radom, Ab Initio Molecular Orbital Theory, Wiley Interscience, New York, 1986, p. 78.
[47] M.J. Frisch, G.W. Trucks, H.B. Schlegel, G.E. Scuseria, M.A. Robb, J.R. Cheeseman, J.A. Montgomery Jr., T. Vreven, K.N. Kudin, J.C. Burant, J.M. Millam, S.S. Iyengar, J. Tomasi, V. Barone, B. Mennucci, M. Cossi, G. Scalmani, N. Rega, G.A. Petersson, H. Nakatsuji, M. Hada, M. Ehara, K. Toyota, R. Fukuda, J. Hasegawa, M. Ishida, T. Nakajima, Y. Honda, O. Kitao, H. Nakai, M. Klene, X. Li, J.E. Knox, H.P. Hratchian, J.B. Cross, C. Adamo, J. Jaramillo, R. Gomperts, R.E. Stratmann, O. Yazyev, A.J. Austin, R. Cammi, C. Pomelli, J.W. Ochterski, P.Y. Ayala, K. Morokuma, G.A. Voth, P. Salvador, J.J. Dannenberg, V.G. Zakrzewski, S. Dapprich, A.D. Daniels, M.C. Strain, O. Farkas, D.K. Malick, A.D. Rabuck, K. Raghavachari, J.B. Foresman, J.V. Ortiz, Q. Cui, A.G. Baboul, S. Clifford, J. Cioslowski, B.B. Stefanov, G. Liu, A. Liashenko, P. Piskorz, I. Komaromi, R.L. Martin, D.J. Fox, T. Keith, M.A. Al-Laham, C.Y. Peng, A. Nanayakkara, M. Challacombe, P.M.W. Gill, B. Johnson, W. Chen, M.W. Wong, C. Gonzalez, J.A. Pople, Gaussian 03 (Revision B.04), Gaussian, Inc., Pittsburgh, PA, 2003.
[48] F. Turecek, J. Phys. Chem. A 102 (1998) 4703.
[49] R. Dennington II, T. Keith, J. Millam, K. Eppinnett, W. Lee Hovell, R. Gilliland, GaussView (Version 3.0), Semichem, Inc., Shawnee Mission, KS, 2003.
[50] M.M. Meot-Ner (Mautner), S.G. Lias, in: P.J. Linstrom, W.G. Mallard (Eds.), NIST Chemistry WebBook, NIST Standard Reference Database Number 69, Gaithersburg, MD 20899, June 2005, http://webbook.nist.gov.
[51] E.G. Robertson, J.P. Simons, Phys. Chem. Chem. Phys. 3 (2001) 1.
[52] I.-S. Hahn, C. Wesdemiotis, Int. J. Mass Spectrom. 222 (2003) 465.
[53] G. Bouchoux, D. Leblanc, W. Bertrand, T.B. McMahon, J.E. Szulejko, F. Berruyer-Penaud, O. Mo, M. Yanez, J. Phys. Chem. A 109 (2005) 11851.
[54] G. Bouchoux, N. Choret, F. Berruyer-Penaud, J. Phys. Chem. A 105 (2001) 3989.
[55] M. Meot-Ner, Chem. Rev. 105 (2005) 213.
[56] D.H. Aue, H.M. Webb, M.T. Bowers, J. Am. Chem. Soc. 95 (1973) 2699.
[57] B. Chan, J.E. Del Bene, J. Elguero, L. Radom, J. Phys. Chem. A 109 (2005) 5509.
[58] J.E. Szulejko, T.B. McMahon, V. Troude, G. Bouchoux, H.E. Audier, J. Phys. Chem. A 102 (1998) 1879.